

Cross section and analyzing power measurements for the giant resonance region in ^{208}Pb with 200-MeV protons

D. K. McDaniels, J. R. Tinsley,* J. Lisantti, D. M. Drake,[†] I. Bergqvist,[‡] and L. W. Swenson[§]
University of Oregon, Eugene, Oregon 97403

F. E. Bertrand, E. E. Gross, D. J. Horen, and T. P. Sjoreen
Oak Ridge National Laboratory, Oak Ridge, Tennessee 37830

R. Liljestrand and H. Wilson
University of Alberta, TRIUMF, Vancouver, British Columbia, Canada V6T 2A3
 (Received 8 July 1985)

The giant resonance region in ^{208}Pb has been studied using inelastic scattering of 200-MeV polarized and unpolarized protons. Both differential cross sections $\sigma(\theta)$ and analyzing power $A_y(\theta)$ measurements were made. The isoscalar giant quadrupole resonance at 10.6 ± 0.5 MeV, and the combined isovector giant dipole resonance and isoscalar giant monopole resonance at 14.0 ± 0.6 MeV are clearly observed. Within uncertainties all three giant resonances are in accord with full energy-weighted sum rule depletions, based on comparisons with macroscopic distorted wave Born approximation calculations. Data for a peak at 20.9 ± 1.0 MeV are found to be consistent with an isoscalar giant octupole resonance exhausting $36 \pm 12\%$ of the energy-weighted sum rule strength. A peak located at an excitation energy of 12.0 ± 0.7 MeV is shown to be a $2\hbar\omega$, $L=4$ transition depleting $8 \pm 3\%$ of the hexadecapole energy-weighted sum rule strength. The measured reduced transition probability for the 3^- state at 2.614 MeV is consistent both with the accepted value and with results measured at 334 and 800 MeV. Our results for the 3^- state at 2.614 MeV and for the giant quadrupole resonance do not support the anomalous behavior found in earlier studies at 104, 156, and 201 MeV. This shows that the macroscopic distorted wave Born approximation can be used to extract deformation lengths providing meaningful comparison with electromagnetic energy-weighted sum rules for proton inelastic scattering to at least 800 MeV incident proton energy.

I. INTRODUCTION

Now that the systematics of giant resonances have become better established, studies of this type are moving toward a phase in which the various giant resonances can be used as a tool to understand other basic aspects of this and related phenomena. This is exemplified by the use of the giant Gamow-Teller resonance to elucidate fundamental questions about beta decay,¹ astrophysics,² and the role of isobar-hole processes³ in various nuclear reactions. Another example is the use of the newly found $M1$ states⁴ to study the energy dependence of the spin-isospin portion of the effective interaction. Measurements of the excitation energy for the giant monopole resonance⁵ (GMR) have provided an experimental determination of the compression modulus of nuclear matter. This in turn is valuable in investigating new phenomena such as superdense matter and in providing a constraint on the hypothesized form of the nuclear force.

Because it is a doubly closed shell nucleus, ^{208}Pb is especially amenable to theoretical analysis. Good wave functions and transition densities exist and microscopic analyses of the excitation of giant resonances by inelastic hadron scattering have proven useful. An essential ingredient of the theoretical studies is knowledge of the location, width, multipolarity, and strength of each giant resonance. The use of a variety of probes is important for this

type of study because the relative strength of excitation of giant resonances through inelastic scattering by electrons, alpha particles, deuterons, and protons may be quite different.

Although the parameters of the isoscalar giant quadrupole resonance (GQR) and the GMR are well established⁶ in ^{208}Pb , the exact location of the $3\hbar\omega$ isoscalar giant octupole resonance (GOR) strength is still controversial. Measurements^{7,8} made with 172-MeV alphas were interpreted as showing excitation of an $L=3$ resonance at 17.5–18.7 MeV. The GOR peak is often partially obscured in (α, α') experiments because of breakup following neutron and proton pickup reactions. Support for a GOR at 17.5 MeV is also given by a recent (p, p') experiment⁹ performed with 201-MeV protons. An experiment with 800-MeV protons¹⁰ reported that the GOR is located near 19.1 MeV, while a 120-MeV ($^3\text{He}, ^3\text{He}'$) measurement¹¹ favored an excitation energy of 20.5 MeV. Clarification of the position of the GOR is essential to the theoretical explanation of isoscalar $E3$ distributions in nuclei, as has been emphasized in a recent schematic model calculation.¹²

A further point of interest concerns the location of isoscalar $L=4$ giant hexadecapole resonance (GHR) strength. For $L=4$ excitations strength is expected in $0\hbar\omega$, $2\hbar\omega$, and $4\hbar\omega$ transitions. Random phase approximation (RPA) calculations^{13–15} indicate that the $2\hbar\omega$ hex-

adecapole strength should be located near the same energy as the $2\hbar\omega$ GQR with an energy-weighted sum rule (EWSR) depletion of 15–40% of the $T=0$, $L=4$ strength in the $2\hbar\omega$ transitions. Inelastic scattering of medium-energy protons provides an excellent approach to search for $L=4$ strength mixed in with the GQR. This ability derives largely from the fact that the angular distributions for $L=2$ and $L=4$ excitations are very different,^{16,17} quite unlike the situation for (α, α') studies. Previous estimates of the $2\hbar\omega$, $L=4$ strength have been obtained by fitting the GQR resonance angular distributions with combined $L=2$ and $L=4$ multipolarities. In the present work evidence is presented for the direct observation of the $L=4$ peak. This study has been reported elsewhere;¹⁸ the emphasis in the present paper is on obtaining a more reliable value of the EWSR.

Theoretical calculations also predict the existence of an isoscalar giant dipole resonance (ISGDR) and an isovector giant quadrupole resonance (IVGQR) in the high excitation region near 25 MeV. The 201-MeV proton data from Orsay⁹ were interpreted as exciting a combined ISGDR and IVGQR at 21.5 MeV, whereas the studies^{7,8} with 172-MeV α particles suggested that a peak found at 21.3 MeV was an ISGDR. A more recent experiment with 340- and 480-MeV alpha particles¹⁹ claims that the $T=0$, $L=1$ strength is concentrated between 26 and 31 MeV of excitation.

It has been reported that a serious problem exists with medium energy proton studies of giant resonances involving the determination of EWSR strengths. The status of EWSR strength determinations for the GQR was summarized recently.²⁰ For proton studies, the GQR sum-rule strength appears to vary from about 80%, obtained from low-energy proton work, to about 30% at 200 MeV. The authors of Ref. 20 conclude that in general EWSR strengths obtained using strongly absorbing particles like ^3He , α , d , and low-energy protons are considerably higher than those obtained employing deeply penetrating particles such as intermediate energy protons. There have been several theoretical suggestions to explain this behavior.^{21,22} It is our belief, however, that this anomaly in the EWSR strengths found for the GQR with medium energy protons is of experimental origin. These experimental difficulties are elaborated upon in the next two sections. Particularly careful attention has been given to the proper evaluation of the continuum background²³ under the giant resonance. To further test the validity of the macroscopic DWBA approach in extracting EWSR strengths, the reduced transition probability for the well-resolved 3^- state at 2.61 MeV has been evaluated and compared with other results at both lower and higher incident proton energies.

Differential cross sections for the excitations of giant resonances in ^{208}Pb by 200-MeV protons were measured at TRIUMF (the variable energy cyclotron facility at the University of British Columbia) as part of our overall program to show the feasibility and utility of medium energy protons as a probe for giant resonance investigations.²⁴ Our measurements cover a large angle range, 6° to 20° , and a large excitation energy range, about 40 MeV. At some angles the cross section data have been supplement-

ed with analyzing power $[A_y(\theta)]$ measurements at 200 MeV. The $A_y(\theta)$ data have proven useful in studying the continuum background.²³

II. EXPERIMENTAL PROCEDURE

All measurements were performed at TRIUMF. The incident proton energy was 200 MeV, with typical beam intensities of 0.1–1.5 nA. The absolute beam intensity was determined by integrating the charge collected on a Faraday cup located downstream from the target position. This charge measurement was checked using a calibrated monitor consisting of proton-proton (p-p) scattering from a thin CH_2 target located well upstream of the target chamber arrangement. The incident protons were scattered inelastically from ^{208}Pb targets that were typically 80 mg/cm^2 thick.

Scattered protons were detected in the TRIUMF broad-range medium-resolution spectrograph (MRS) facility. The spectrograph, which consists of a quadrupole and dipole magnet, bends scattered particles vertically out of the scattering plane. Since the spectrograph has a very large acceptance of $\pm 10\%$ in momentum, most of our spectra cover an excitation energy range of about 40 MeV for a single magnetic field setting. The spectrograph can be rotated to measure angular distributions over the range of 2.5 – 135 deg.

During the course of this experiment the MRS was operated in two very different configurations. Initially, the cyclotron beam was focused to a small area on the targets located in the scattering chamber. The scattered particles then passed through a thin plastic scintillator mounted in front of the spectrograph and a thicker plastic scintillator located well beyond the focal plane. The fast scintillator pulses were used in a time-of-flight identification system. The trajectory of the scattered particles was determined by signals from a 12.5-cm by 12.5-cm wire chamber located in front of the magnets and two large multiwire proportional chambers after the magnets. The front wire chamber also determined the angular acceptance of the spectrograph, allowing determination of absolute cross sections. The combined energy resolution of the cyclotron, beam transport system, and spectrograph was usually about 1 MeV full-width at half maximum (FWHM). Most of our data were obtained in this configuration.

A typical spectrum obtained with this configuration is presented in Fig. 1. Because of poor resolution, the low lying states, with the exception of the state at 2.614 MeV, were not well resolved so that determination of the best continuum background to subtract out was difficult. The background subtraction procedure used is described in more detail below. The scattering chamber used in this operating mode limited our maximum scattering angle to 20° . True zero in scattering angle was found by comparing our elastic-scattering angular distributions with the results of a precise experiment on ^{208}Pb .²⁵

Recently the MRS facility was upgraded to high resolution operation. In order to reduce the contribution of the cyclotron beam energy spread to the resolution, a six-quadrupole beam phase-space twister was installed

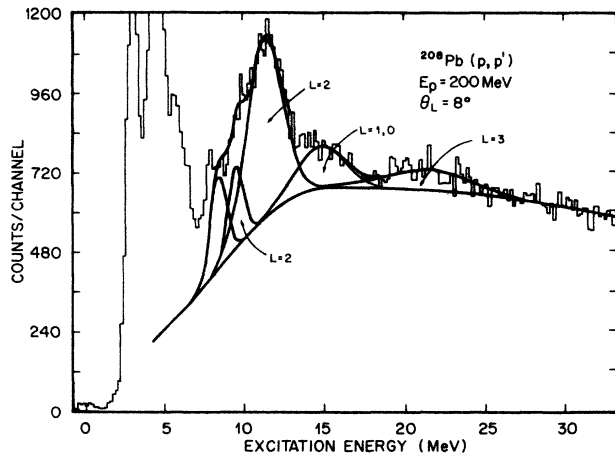


FIG. 1. Spectrum of 200-MeV unpolarized protons scattered from a ^{208}Pb target at a laboratory angle of 8° . Decomposition of spectra into peaks was done with the least squares fitting program MINUIT. This spectrum was obtained with the MRS in a low resolution configuration so that FWHM for the elastic peak was of the order of 1000 keV.

upstream of the spectrograph target location. This system rotates the beam momentum dispersion from the horizontal to the vertical plane to allow matching to the dispersion of the spectrograph. A new target chamber was also constructed which provides a continuous vacuum from the beam line through the spectrograph. The only device now located in front of the MRS is a low pressure wire chamber, specially designed to minimize the amount of material through which the scattered beam must pass. Finally, two new vertical drift focal plane chambers with a spatial resolution of $100\ \mu\text{m}$ were installed. The improvement in the spectra obtained with the new MRS configuration is strikingly illustrated in Fig. 2. The effective resolution for these data was 160 keV.

A feature of both MRS configurations is that each particle is traced back to the point of origin on the target. Placing cuts on the target then allowed us to eliminate events arising from such things as pole face scattering, etc. This is a particularly important feature for the new MRS configuration. The much improved resolution obtained with the new MRS configuration made it easier to establish the continuum background under the giant resonance peaks.

Elimination of spurious backgrounds due to scattering from beam pipes, magnet frame, etc., is a major concern. In our case this background was eliminated in the region of interest by carefully tuning the beam line transport magnets and by properly centering the beam on the target. Checks were made for bogus background at forward angles using empty target frames. Spectra measured at zero degrees to study the cleanness of the beam also allowed us to determine the response of the spectrograph across the entire focal plane.

Absolute differential cross sections were determined from the integrated beam current, target thickness, and spectrograph acceptance solid angle. As a check on our cross section determination, the elastic scattering of 200-

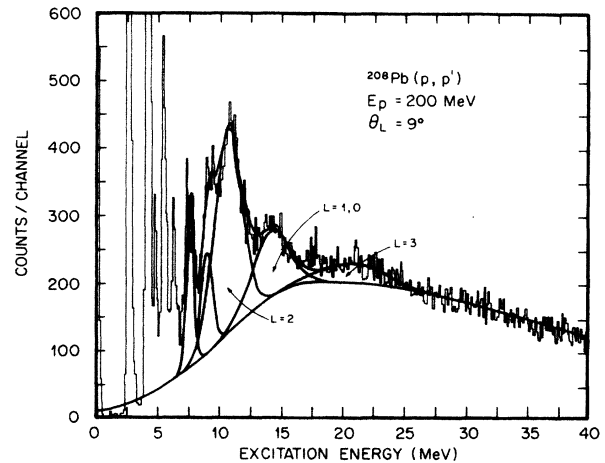


FIG. 2. High-resolution spectrum for 200-MeV unpolarized protons scattered from a ^{208}Pb target at 9° . The FWHM for low-lying peaks is about 160 keV. See the text for details of the MRS in this dispersed mode configuration.

MeV protons on a CH_2 target was measured and compared with the accepted cross section values.²⁶ On the average our measured p-p cross sections were within $\pm 6\%$ of the standard values obtained from the phase-shift calculations. In addition, the values of the ^{208}Pb elastic-scattering cross sections measured in this experiment were compared with the precise TRIUMF values²⁵ at 200 MeV; agreement to within $\pm 7\%$ was obtained.

It is extremely important to have good measurements of the angular distributions of the differential cross sections

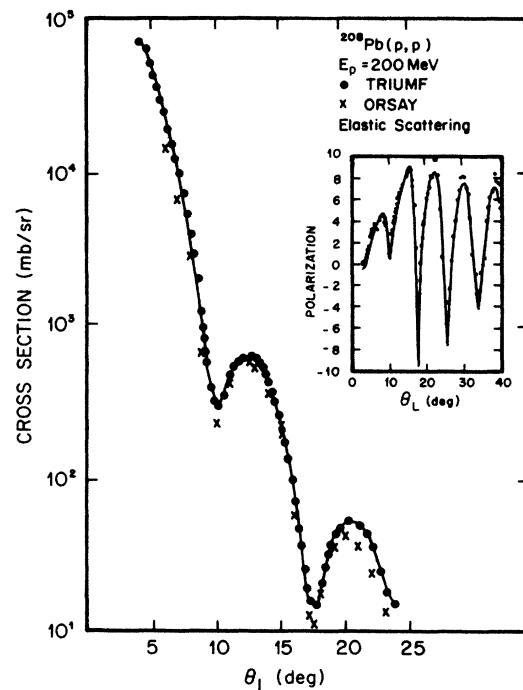


FIG. 3. Elastic scattering data used to obtain our optical model parameters. The solid circles are points from Ref. 25.

TABLE I. Optical model parameters for ^{208}Pb (RSO denotes real spin orbit).

$V_R = 11.17$ MeV	$V_I = 21.17$ MeV	$V_{\text{RSO}} = 2.20$ MeV	$V_{\text{ISO}} = -2.86$ MeV
$r_R = 1.32$ fm	$r_I = 1.15$ fm	$r_{\text{RSO}} = 1.10$ fm	$r_{\text{ISO}} = 1.06$ fm
$a_R = 0.60$ fm	$a_I = 0.80$ fm	$a_{\text{RSO}} = 0.69$ fm	$a_{\text{ISO}} = 0.80$ fm
$r_C = 1.20$ fm			

and polarization for elastic scattering at 200 MeV. It was found that cross sections calculated in the DWBA approximation²⁷ using collective form factors were quite sensitive to the optical model parameters used to generate the distorted waves. The forward angle elastic scattering data²⁵ used to determine our optical model parameters are shown in Fig. 3. The optical model parameters are summarized in Table I. Also shown in Fig. 3 are the elastic scattering data from the Orsay experiment.⁹ Their elastic scattering results are lower than the TRIUMF measurements.

The availability of a high-quality polarized beam allowed us to supplement the differential cross section data with analyzing power measurements. In terms of the polarization (P_{\uparrow} and P_{\downarrow}) of the incident beam, the analyzing power can be written as

$$A_y(\theta) = \frac{\sigma_{\uparrow}(\theta) - \sigma_{\downarrow}(\theta)}{P_{\uparrow}\sigma_{\uparrow}(\theta) - P_{\downarrow}\sigma_{\downarrow}(\theta)}. \quad (1)$$

Beam polarization, as obtained with an in-beam polarimeter, varied from 0.72 to 0.75 from one measurement to the next. The uncertainty of an individual determination was ± 0.005 , whereas the larger variation between runs was due to changing ion source conditions. Data with unpolarized beam incident on a ^{208}Pb target in the low resolution MRS mode were taken for angles between 6° and 20° in 2° steps, whereas those with polarized beam ranged between 6° and 14° in 2° steps. High resolution data were taken at 5, 7, 9, 11, 13, and 15 deg.

Decomposition of the measured spectra into individual giant resonance peaks is an important and subjective procedure. The major problem involves the estimation of the background under the resonances. We have adopted a procedure in which the continuum background is described as a Gaussian for inelastic protons with energies higher than that corresponding to the peak associated with quasifree NN scattering.²³ The background above this point (lower energy protons) was described by a fourth order polynomial drawn smoothly through the data.

The final decomposition of the giant resonance peaks was done with the aid of the peak fitting program MINUIT.²⁸ The stripping procedure consisted of first determining a reasonable fit to the underlying continuum for excitation energies above the energy associated with quasifree kinematics using a fourth order polynomial. The background for excitation energies below the energy associated with quasifree scattering was determined empirically using the Gaussian form

$$N = N_0 e^{-(E - E_0)^2/\lambda}, \quad (2)$$

with N_0 being the value of the polynomial fit at the quasi-

free centroid. The width parameter λ was established from analysis of our high resolution spectra for ^{208}Pb and ^{60}Ni . The experimental width values are plotted in Fig. 4. The straight line on this figure is the result of Monte Carlo calculations²⁹ for a Fermi momentum equal to 230 MeV. We observe that the width of the Gaussian increases with angle. Once the background was established the individual giant resonance peaks were fitted in a least squares sense using a Gaussian shape for all peaks. Locations and widths of the different giant resonance peaks were determined at angles where the various multipolarity peaks were maximized in cross section. These peak parameters were then fixed for analysis at all other angles.

It must be emphasized that our background subtraction procedure does not rest solely upon the quasifree scattering hypothesis. We do believe that for low excitation energies this is the dominant background process based²³ on the observed kinematical shifting of the continuum peak with scattering angle and of the approximate equality of $A_y(\theta)$ in the region of the continuum peak and $A_y(\theta)$ values for free NN scattering. However, our background was not determined from any theoretical calculation assuming the quasifree hypothesis.

Instead our background procedure is an empirical one

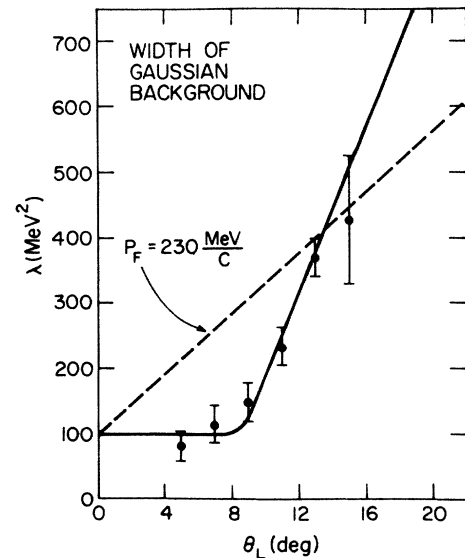


FIG. 4. The measured width parameters for our assumed Gaussian background distribution are plotted as a function of laboratory angle. The solid circles were obtained from our high resolution spectra. The dashed line was obtained from a Monte Carlo calculation with a Fermi gas momentum distribution. The ordinate is explained in the text.

based on a criterion of reasonableness. Our high resolution spectra (see Fig. 2) show an approximate Gaussian falloff as the excitation energy decreases from the energy associated with a quasifree process. Further justification for this comes from the calculated shape of the Monte Carlo spectra at high proton energies. These calculations were done using measured NN cross sections that include all physical processes. While we believe that the background scattering processes in this low excitation region are dominated by the quasifree process, our assumed Gaussian shape is based primarily on the appearance of the background in our high resolution spectra.

Cross section obtained from the high resolution measurements are not dependent upon using a Gaussian background in the low excitation region. The more customary procedure of drawing in the most reasonable shape for the background yields almost identical results. The low resolution data are naturally quite sensitive to the choice of background. Using the Gaussian shape and measured width parameters (see Fig. 4), the giant resonance cross sections deduced from the low resolution work are in essential agreement with those deduced from the high resolution measurements. Cross sections measured for the low lying excited state at 2.614 MeV where the background contribution was almost negligible are not affected by the above considerations as all data were acquired in either the high resolution (160 keV) or medium resolution (450 keV) mode.

III. RESULTS

A measurement of the angular distribution of the 2.614 MeV, 3^- state of ^{208}Pb serves as a useful check on the validity of the macroscopic DWBA calculations. Good data were obtained from the giant resonance measurement with 160 keV resolution and also from an earlier special measurement with the older MRS configuration and a dedicated cyclotron. Both sets of data agreed within uncertainties, and the combined data are shown in Fig. 5 along with the results of a DWBA calculation using a deformation length of $\beta_3 R = 0.75$. Our estimate of the uncertainty in $\beta_3 R$ is ± 0.03 . The DWBA calculations were made with the code ECIS 79 which utilizes a full Thomas form³⁰ for the spin orbit part of the optical potential. The deformation length ($\beta_i R_i$) was kept constant³¹ throughout all terms of the optical potential (and the collective interaction) including the spin orbit terms. The measured deformation length required to fit the data was then converted to a reduced transition probability using the relation

$$B(EL) = \left[Z \int \rho_{\text{tr}}(r) r^{L+2} dr \right]^2 = \left[Z \frac{(L+2)}{4\pi} (\beta_L R) \langle r^{L-1} \rangle \right]^2. \quad (3)$$

The transition density is assumed to be proportional to $(\beta_L R)$ and the derivative of the density, which holds for surface vibrational models. The factor Z is included, rather than A , in order to ensure approximate equality³² of the hadronic and electromagnetic matrix elements. For a uniform distribution the above simplifies to

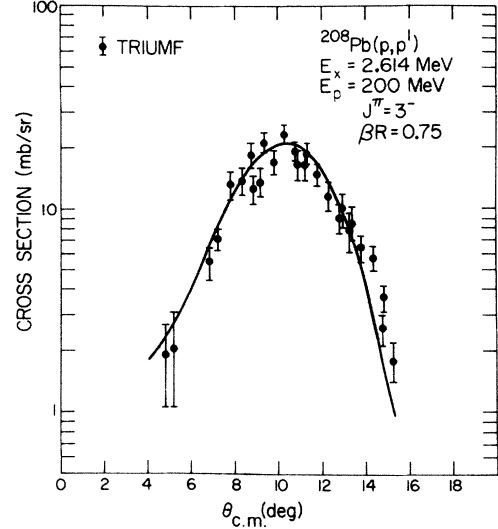


FIG. 5. Angular distribution for the 3^- state at 2.614 MeV. The best DWBA fit corresponds to a deformation length of $\beta R = 0.75$ for all parts of the optical potential.

$$B(EL) = \left[\frac{3Z}{4\pi} \right]^2 (\beta_L R)^2 R^{2L-2}. \quad (4)$$

All of our reduced transition probabilities were calculated using this result. For ^{208}Pb , the uniform distribution reduced transition probabilities agree quite well with values calculated using a more precise evaluation of the radial moments.³³

For our 200-MeV data, $B(E3) = (5.5 \pm 0.4) \times 10^5 e^2 \text{ fm}^6$, using $\beta_3 R = 0.75 \pm 0.03$ and $R = 1.20A^{1/3}$. This compares well with the presently accepted value of $(6.11 \pm 0.13) \times 10^5 e^2 \text{ fm}^6$ obtained primarily from electromagnetic (e, e') measurements.³⁴ Thus, the macroscopic collective model DWBA calculations appear to satisfactorily describe the results for the scattering of 200-MeV protons to the low-lying 2.614-MeV state of ^{208}Pb . This point is elaborated upon below in the discussion section where the present results for 200-MeV protons are compared with $B(E3)$ values for incident protons at other energies.

As shown in Figs. 1 and 2, the most prominent feature observed in the inelastic ^{208}Pb spectra measured with 200-MeV protons is a broad distribution rising above the continuum and centered near 11 MeV. At 8° the peak fitting procedure was most consistent with a decomposition of this broad feature into peaks at 7.9, 8.9, 10.6, and 14.0 MeV. At larger angles it was necessary to include an additional peak at 12.0 MeV. This is quite clearly seen in Fig. 6, which shows the spectrum at 13° , where the peak at 12.0 MeV is identified as $L = 4$ strength.

Giant resonance cross sections for the various peaks were extracted following the procedure outlined in the preceding section. The results for the giant quadrupole peak (GQR) at 10.6 MeV are presented in Fig. 7. The points at the odd angles represent results obtained from the high resolution measurements. Within uncertainty the

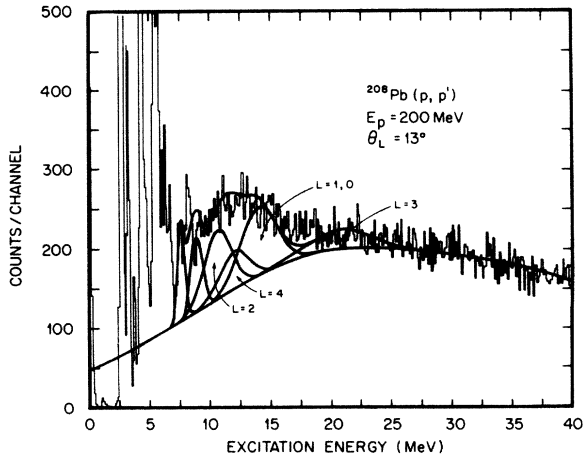


FIG. 6. High resolution spectrum for 200-MeV unpolarized protons scattered from a ^{208}Pb target of 13° . The FWHM for low-lying peaks is about 160 keV.

high resolution data are in agreement with the earlier results obtained at low resolution. The solid curve shows a DWBA calculation with a normalization corresponding to 65% of the theoretical sum rule,¹⁷

$$(\beta_L R)^2 = \left[\frac{2\pi\hbar^2}{3m} \right] \frac{L(2L+1)}{AE_x}. \quad (5)$$

All of the DWBA calculations for $L > 1$ were made with a collective form for the transition potential,

$$U_L(r, \Omega) = \frac{\beta_L R}{\sqrt{2L+1}} \frac{dU_0(r)}{dr} Y_{L0}(\Omega), \quad (6)$$

involving the derivative of the optical potential, $U_0(r)$. The experimental value for $\beta_L R$ was obtained by comparing the data with the results of the DWBA calculation using a $\beta_L R$ corresponding to 100% depletion of the EWSR. Explicitly we have that

$$\frac{(\beta_L R)_{\text{expt}}^2}{(\beta_L R)_{100\%}^2} = \frac{\sigma_{\text{measured}}}{\sigma_{\text{DWBA}}}. \quad (7)$$

This value of $\beta_L R$ was then used to obtain the solid curve shown in Fig. 7. In our DWBA calculations, βR was kept constant in each of the individual terms in the transition potential ($\beta_R R_R = \beta_I R_I = \beta_{so} R_{so}$), just as for the 3^- state.

It can be seen from Fig. 7 that the GQR data are con-

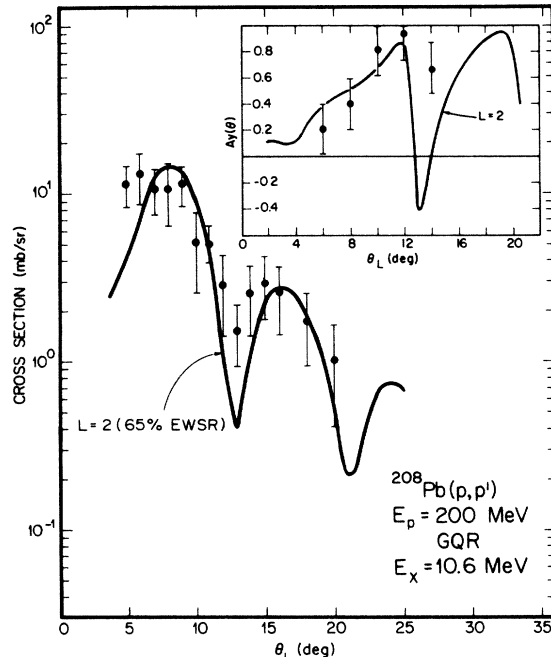


FIG. 7. Angular distribution for the GQR strength at 10.6 MeV of excitation. The solid circles are the absolute cross sections measured with the TRIUMF spectrograph. The solid curve is the DWBA prediction for $L=2$ excited with a strength of 65% of the EWSR. The inset shows our measured $A_y(\theta)$ data along with the DWBA calculation.

sistent with the DWBA calculation within the uncertainties of the data. These uncertainties come from the background subtraction. $A_y(\theta)$ data for the GQR peak at 10.6 MeV are shown in the inset to Fig. 7. Agreement with the $L=2$ DWBA predictions is satisfactory, but the data quality is insufficient to allow any study of the sensitivity to spin-orbit parameters.³¹ The results from the present measurements for the GQR are summarized in Table II. The values for the centroid and width compare well with other (p,p') measurements.^{9,20,35} Our observed EWSR depletion of $65 \pm 15\%$ agrees generally with both the low energy proton results⁶ and the (α, α) strengths,^{7,8} is in sharp disagreement with other proton results at 104 MeV (Ref. 20) and at 201 MeV (Ref. 9), but agrees with another measurement by our group made with incident protons of 334 MeV.³⁶

TABLE II. Comparison of giant resonance parameters.

J^π	T	E_x (MeV)	Present results		Ref. 9 (p,p')		$(\alpha, \alpha')^a$	
			Γ (MeV)	EWSR (%)	E_x (MeV)	EWSR (%)	E_x (MeV)	EWSR (%)
(2,3)	0	8.9 ± 0.6	1.2 ± 0.6	8 ± 5	9.0	7 ± 1		
2^+	0	10.6 ± 0.5	2.4 ± 0.6	65 ± 15	10.6	24 ± 3	10.9 ± 0.3	60 ± 10
4^+	0	12.0 ± 0.7	2.5 ± 1.0	8 ± 3	≈ 11	6	12.5	14
1^-	1	14.0 ± 0.6	3.4 ± 0.8	100 ± 30	13.5	100	13.8	90
0^+	0				13.9	25 ± 10		
3^-	0	20.9 ± 1.0	5.9 ± 1.0	36 ± 12	17.6		17.5 ± 0.8	60

^aSee Refs. 7 and 8.

Consistently visible in the low excitation portion of the spectra are two peaks at 7.8 ± 0.5 and 8.9 ± 0.6 MeV. The peak at 7.9 MeV was too poorly resolved to analyze at all angles, but its angular distribution was consistent with a multipolarity of either $L=2$ or 3. Similarly, the cross section data for the 8.9 MeV state are consistent with either $L=2$ or 3. Our cross section values are in accord with the value of 7% EWSR ($L=2$) for the 8.9-MeV peak found in the 201-MeV studies.⁹ This study also reported on peaks at 8.9 and 9.3 MeV with multiplicities of $L=2$ and $L=3$, respectively. Earlier (α, α') studies⁷ reported $L=4$ peaks at 7.4 and 8.1 MeV. More recent alpha particle inelastic scattering studies⁸ found no evidence for a peak at 8.9 MeV, but reported on an $L=3$ peak at 9.3 MeV. Our results at 334 MeV are consistent with the excitation of 2^+ states at 7.36, 7.84, 8.86, and 9.34 MeV. The sum of the $L=2$ strength found in these states is about 20%. Coupled with the 9% of the $L=2$ strength for the excitation of the 2^+ state at 4.086 MeV, it is seen that almost 30% of the $L=2$ strength is found in states below 10 MeV.

Another feature of our spectra involves the excitation of the GDR and GMR giant resonances. In the analysis of our spectra the GDR and GMR excitations were analyzed together as one peak centered at 14.0 MeV. Extraction of cross sections was done using the analysis program MINUIT and a Gaussian shape for the combined peaks. The cross section results are shown in Fig. 8.

In the DWBA calculation for the GDR the transition potential was taken as proportional to the derivative of the isovector part of the optical potential, along with a term accounting for Coulomb excitation.¹⁷ Calculations were performed with two different values of V_1 , as shown in Fig. 8. The value of 25 MeV corresponds to the result obtained from optical model analyses of low energy

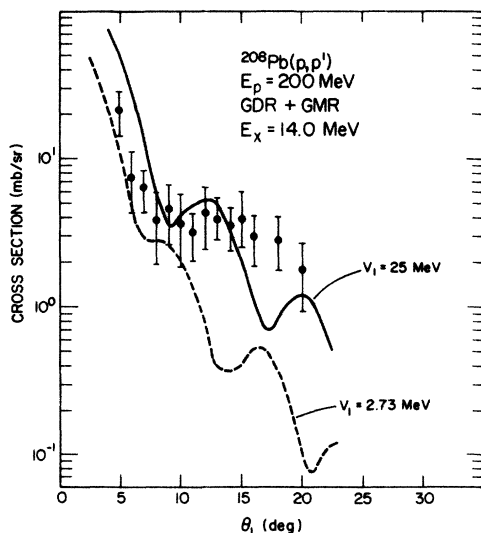


FIG. 8. Measured angular distribution for the peak located at the excitation energy of 14.0 MeV, assumed to be a combined $T=1$ GDR and $T=0$ GMR. The curves show DWBA predictions for the combined peak assuming 100% EWSR for the GMR and two different values of V_1 .

nucleon-nucleus scattering.³⁷ A more recent analysis³⁸ of proton elastic scattering over the range of 60–180 MeV yields $V_1 = 59(1 - 0.18 \ln E_p)$, giving $V_1 = 2.73$ MeV for our case. For the GMR the transition potential used is shown as³⁹

$$xU_0(r) + R \frac{dU_0(r)}{dr}, \quad (8)$$

where $x = (3 + y_m^2)/(1 + y_m^2)$, with $y_m = \pi a_m/R_m$. Normalization for 100% depletion of the EWSR was done using

$$(\beta_0 R)^2 = \left[\frac{2\pi\hbar^2}{3m} \right] \frac{5}{AE_x}. \quad (9)$$

The GDR and GMR calculations assuming full EWSR depletions were then added together and plotted as shown in Fig. 8. It would appear that a value for V_1 of about 15 MeV would best fit the data for angles less than 12–14 deg. For larger angles the data appear to require more than just $L=0$ and $L=1$ strength. It has been suggested¹⁵ that the cross section behavior at larger angles could be improved through the admixture of some $L=4$ strength. Our results are in agreement with these microscopic predictions.

In addition to the well-known 3^- state at 2.614 MeV, the existence of other localized octupole strength has been confirmed.⁶ The $1\hbar\omega$ low-energy octupole resonance (LEOR) has been found to occur systematically at roughly $30A^{-1/3}$ MeV.⁴⁰ Evidence for a higher energy $3\hbar\omega$ GOR with strength concentrated at about $120A^{-1/3}$ MeV comes from inelastic-scattering experiments with electrons,⁴¹ alpha particles,⁷ ^3He particles,¹¹ and protons.^{9,10,24} In the case of ^{208}Pb , although all of the experiments are in rough agreement that the $T=0$, $L=3$ giant resonance is localized near 20 MeV of excitation energy (in agreement with RPA calculations),⁴² there is no consistent agreement about the precise location. The values span the region of 16–21 MeV in excitation.

Our analysis indicates the existence of a broad peak centered at about 20.9 ± 1.0 MeV with a width of about 5.9 ± 1.0 MeV. This peak stands out very clearly in the 8° and 9° spectra, as shown in Figs. 1 and 2. The angular distribution measured for this peak is shown in Fig. 9, with $A_y(\theta)$ data presented in the inset on this figure. The data for the 20.9-MeV peak are reasonably well described by the DWBA calculations as an isoscalar GOR, with an EWSR depletion of 36%. Also shown is a DWBA calculation for $L=2$. Our spectra and cross section results support the $L=3$ strength being located in the region near 21 MeV, rather than at a lower excitation energy as reported in some alpha particles^{7,8} and proton⁹ inelastic scattering studies.

An important advantage of working with 200-MeV protons is the strong differentiation between the angular distributions for neighboring multipoles. These angular distribution differences provide the sensitivity needed to

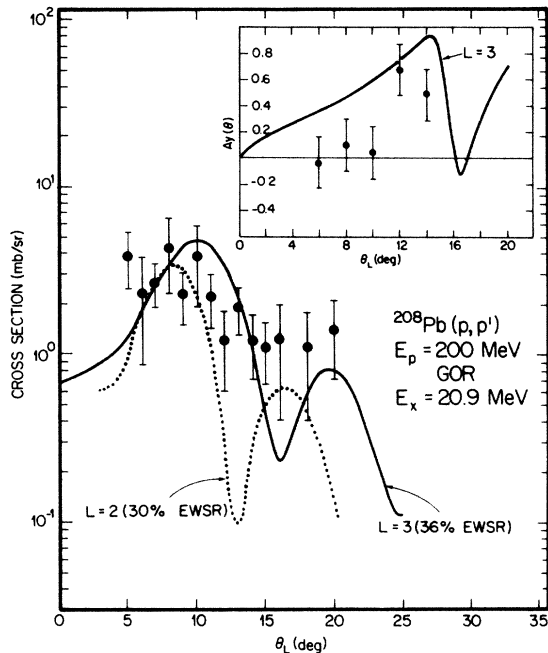


FIG. 9. Angular distribution for the giant resonance peak located at 20.9 MeV of excitation. The solid curve is the prediction of the collective DWBA theory for an $L = 3$ transition. The inset shows our measured $A_y(\theta)$ data along with a DWBA calculation for a multipolarity of $L = 3$.

search for the presence of possible $L = 4$ strength in the region of the GQR peak. Theoretical calculations^{13,14} show a concentration of $2\hbar\omega$, $L = 4$ strength in this region. Some indirect experimental evidence for this strength has been suggested by (α, α') measurements^{8,43} as

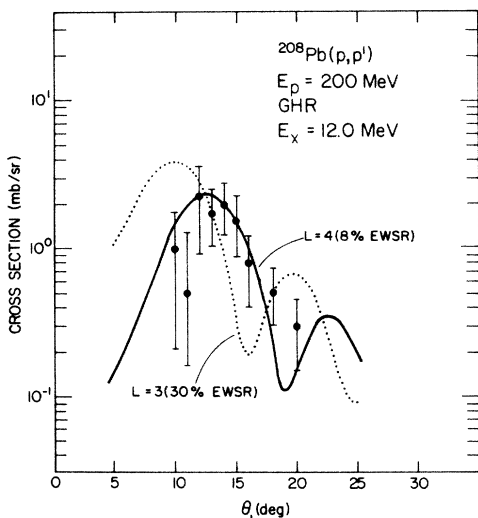


FIG. 10. Experimental angular distribution for the peak at 12.0 MeV. The solid curve is the DWBA prediction for an $L = 4$ excitation depleting 8% of the EWSR. Also shown is the DWBA prediction for an assumed $L = 3$ excitation of 12.0 MeV (dotted curve).

well as proton inelastic scattering experiments.^{9,20,24} However, all of these studies estimated the $L = 4$ strength by determining the amount of $2\hbar\omega$, $L = 4$ strength needed to optimize the agreement between the GQR angular distributions and the DWBA predictions.

As is shown in Fig. 6, we have found it necessary to include a peak at 12.0 MeV to satisfactorily describe the observed spectra for $\theta_L > 12^\circ$. The GQR peak at 10.6 MeV is weakly excited at this scattering angle, and inclusion of a peak centered near 12.0 MeV of excitation is needed to fit the observed data. Whenever possible we have extracted cross sections for the $L = 4$ candidate peak. The measured angular distribution for this peak is shown in Fig. 10 along with DWBA predictions for $L = 4$ and $L = 3$ strength. The solid curve corresponds to the $L = 4$ prediction with an EWSR depletion of 8%. At angles less than 10° the strength of the $L = 4$ peak is too weak compared to the GQR for cross sections to be extracted. Further details about this $L = 4$ strength are given elsewhere.¹⁸ Similar results were obtained with 334-MeV protons.³⁶

IV. DISCUSSION

In agreement with earlier studies, we found a strong isoscalar quadrupole transition concentrated at an excitation energy of 10.6 ± 0.5 MeV. The $L = 2$ character of the strong GQR was corroborated by our $A_y(\theta)$ measurements. Our values for the excitation energy and width, tabulated in Table II, are in good accord with other studies. As is the case in other hadronic experiments, we find no evidence for the fine structure evident in (e, e') studies.⁴¹ Our value for the EWSR of $65 \pm 15\%$ is in general agreement with low energy (p, p') and (α, α') results,^{7,8} and with our results³⁶ obtained with 334-MeV protons. This value would be expected, since about 30% of the $L = 2$ strength is to be found in the lower-lying states.³⁶ The present value for the EWSR for the peak at 10.6 MeV disagrees with the low results obtained for the GQR in other (p, p') studies^{9,20,24,35} at medium energies. These studies might have had difficulties with background subtraction and normalization. For example, the background subtraction procedure for the 156-MeV experiment³⁵ and for the experiment²⁴ on ^{90}Zr and ^{120}Sn at 200 MeV consisted of drawing a straight line for the continuum under the giant resonances. The measurements⁹ at 201 MeV may have had difficulties with absolute normalization inasmuch as their elastic scattering data were also low. We have also found that our results are quite sensitive to the choice of optical parameters. Great care has been taken to adjust the optical parameters so that good agreement with the precise data²⁵ at 200 MeV was obtained.

Our cross section data for the 20.9-MeV peak are consistent with an interpretation as an isoscalar GOR. The $A_y(\theta)$ results suffer from large uncertainties in the data. $A_y(\theta)$ measurements, while of considerable usefulness for studies of the continuum background,²³ appear to be of limited utility for the giant resonance investigations unless extremely good statistics are obtained. A GOR with a width of about 5.3 MeV was found at 19.1 ± 1.0 MeV in an inelastic proton-scattering experiment¹⁰ at 800 MeV

and at 20.5 MeV in ^3He -scattering studies.¹¹ RPA calculations^{13,15,44} predict an $L=3$ resonance of 20.1 MeV with a width of 5.9 MeV, in good agreement with the present result. Our result, putting the location of the GOR peak at about 21 MeV, is in disagreement with the proton experiment⁹ at 201 MeV and with the 172-MeV alpha-scattering results.^{7,8} The EWSR depletion of $36 \pm 12\%$ found in the present experiment agrees very well with the value predicted by RPA calculations.^{13,44} The recent high statistics (α, α') study¹⁹ observes 3^- strength rather uniformly distributed from about 17 to 35 MeV of excitation.

Evidence is found for resonance strength at 12.0 ± 0.3 MeV in ^{208}Pb . The angular distribution for this peak is consistent with an $L=4$ $2\hbar\omega$ excitation, with an EWSR depletion of $8 \pm 3\%$. We have previously used²⁴ the inelastic scattering of 200-MeV protons to get an upper limit on the amount of $L=4$ strength present in the GQR region of ^{90}Zr and ^{120}Sn . The sensitivity of these measurements arises from the fact that where the cross section for $L=2$ excitations is at minimum, the cross section for $L=4$ excitations is at maximum. Additional inferred evidence for $L=4$ strength has been obtained from (α, α') inelastic scattering^{7,8,45} and from 115-MeV proton inelastic scattering by ^{92}Zr .⁴⁶ The present result is distinct from earlier studies in that a definite peak was observed at 12.0 MeV, near the location of the GQR. The location, width, and strength of this $2\hbar\omega$ GHR for ^{208}Pb are in excellent agreement with recent calculations.^{14,16} Observation of the $2\hbar\omega$ GHR in nuclei lighter than ^{208}Pb will be more difficult because the width is smallest for the case of lead and increases as $A^{-2/3}$. Based only on the present results for ^{208}Pb and on the observation of a similar excitation¹⁸ of the $2\hbar\omega$ in ^{206}Pb , the resonance may be expected to be located at the systematic energy of $70A^{-1/3}$ MeV.

Microscopic calculations predict the existence of a $3\hbar\omega$ isoscalar dipole mode. According to RPA calculations⁴⁷ this $T=0$, $L=1$ strength [$3\hbar\omega$ compression mode excited by an operator proportional to $r^3 Y_{10}(\Omega)$] should lie between 23 and 29 MeV of excitation. It was claimed from the studies with 201-MeV protons⁹ that their data at small angles were consistent with Coulomb excitation of an IVGQR mode while their data at larger angles were consistent with an additional ISGDR component. The Saclay (α, α') data¹⁹ were interpreted to support 1^- strength at higher energies between 26 and 35 MeV of excitation. Our large angle data are most consistent with the excitation of 3^- strength. We do not rule out the possibility of other multipole strength being excited at small angles.

Measurements with low energy probes show that for heavier nuclei the GQR is excited with a strength⁶ sufficient to deplete the corresponding theoretical energy-weighted sum rule. Similar results were obtained with higher energy, strongly absorbing probes such as alpha particles.^{7,8} The most important finding of the present study is that the EWSR depletion for the GQR is in accord with the lower energy results. This is in sharp disagreement with the results of other studies with medium energy protons. An anomalous behavior was first reported in a survey experiment in which 156-MeV protons³⁵ were inelastically scattered by targets from ^{27}Al to

^{209}Bi . Using a collective DWBA analysis of the GQR cross sections, the authors of this study reported EWSR strengths for the heavier targets which were less than one-half of the low energy values. Our own early experiment²⁴ at TRIUMF with 200-MeV protons reported low EWSR depletions for the excitation of the GQR in ^{90}Zr and ^{120}Sn . A similar anomalously low EWSR depletion for the GQR in ^{208}Pb was found in the proton scattering experiments at 104 (Ref. 20) and 201 (Ref. 9) MeV. It was noted²⁰ that the EWSR strength for excitation of the GQR in ^{208}Pb goes from about 70% at low incident proton energies to about 30% at 200 MeV. It was their observation that this anomalous behavior was due to the fact that the more penetrating higher energy protons were not being properly described by the surface peaked collective DWBA formalism. The present results, coupled with that for the GQR at 334 MeV,³⁶ lead us to believe that this anomalous behavior for medium energy protons has disappeared. The problems with the earlier measurements were probably due to some combination of difficulties with absolute normalization, background subtraction, and inappropriate optical model parameters.

Early on, this purported anomalous behavior of the EWSR depletion for the GQR stimulated theoretical interest. It was stressed by Madsen *et al.*⁴⁸ at the 1982 conference on giant resonance phenomena at Oak Ridge National Laboratory that the most likely resolution of the problem was that deformation lengths extracted from a collective DWBA analysis of higher energy inelastic proton scattering could no longer be compared directly with a theoretical sum rule derived assuming a transition operator of the form $r^L Y_M^L(\Omega_r)$.

A detailed microscopic calculation of medium energy proton inelastic scattering was made by Osterfeld *et al.*²¹ As a test of the hadronic transition operator in the collective DWBA approach, Osterfeld *et al.* analyzed "data" with a standard DWBA program for several incident proton energies up to 156 MeV. The data for this comparison consisted of inelastic cross sections for the excitation of the 2.614-MeV 3^- state in ^{208}Pb at the various proton energies calculated using RPA transition densities. Confidence in the validity of this approach using RPA wave functions stems from the fact that the excitation of giant resonances arises mainly from a one-body transition operator. The giant resonance states themselves are comprised dominantly of 1p-1h components⁴⁹ which have large transition amplitudes for transitions to the ground state. More complicated 2p-2h components are not expected⁵⁰ to contribute much to the reduced transition probability for the excitation of giant resonances, contributing rather to the spreading width of the state.

Results from the above calculation showed a striking dependence of $B(E3)$ for the 2.61-MeV state as a function of incident proton energy. The $E3$ reduced transition probability extracted from their "data" with the collective DWBA program was found to decrease with energy. At 156 MeV $B(E3)$ was down by roughly a factor of 2 from the low-energy EM value³⁴ of $6.11 \times 10^5 e^2 \text{fm}^6$. The conclusion was drawn that this shows the impropriety of using the collective DWBA formalism to extract deformation parameters for reactions involving deeply penetrating

TABLE III. Reduced transition probabilities for the 2.614 MeV 3^- state in ^{208}Pb .

Incident proton energy (MeV)	Deformation length (βR)	$B(E3)$		Ref.
		$e^2 \text{ fm}^6 \times 10^5$	$\frac{B(E3)_{\text{EM}}}{B(E3)_{\text{expt}}}$	
EM	0.790 ± 0.008	6.11 ± 0.13	1.00	Ref. 34
104	$0.67 \pm 0.02^{\text{d}}$	4.4 ± 0.2	1.40 ± 0.07	Ref. 20
135	0.77 ± 0.06	5.8 ± 0.8	1.05 ± 0.15	Ref. 52
156	$0.77 \pm 0.06^{\text{c}}$	5.8 ± 0.9	1.06 ± 0.17	Ref. 53
200	0.75 ± 0.03	5.5 ± 0.4	1.11 ± 0.08	Present work
201	$0.57 \pm 0.02^{\text{e}}$	$3.2 \pm 0.2^{\text{a}}$	1.89 ± 0.14	Ref. 9
334	0.83 ± 0.04	6.8 ± 0.7	0.91 ± 0.10	Ref. 36
800	0.755 ± 0.064	5.6 ± 1.0	1.09 ± 0.19	Ref. 10
800	0.825 ± 0.025	$6.7 \pm 0.4^{\text{b}}$	0.92 ± 0.06	Ref. 33

^aThe variance of the three different results obtained using the different sets of optical parameters was computed. The uncertainty stated above is equal to this variance.

^bAn uncertainty is βR of 3% was assumed, corresponding to the authors statement about searches on optical parameters.

^c βR extracted from the author's fit using a $B(E3)$ equal to 32 W.u.

^d βR extracted from the author's stated $B(E3)$ of 24.1 ± 1.2 W.u.

^eThe deformation length tabulated was extracted using the average $B(E3)$ from Ref. 9 and Eq. (4). However, we have also reanalyzed the 201-MeV data by renormalizing the 3^- data by the ratio of our 200-MeV elastic scattering cross sections to those measured at 201 MeV. When this is done and a DWBA analysis made using our optical parameters, a value of $\beta R = 0.77$ is obtained.

probes such as medium energy protons.

The present 3^- result at 200 MeV is in disagreement with the above theoretical analysis. Our value of $(5.5 \pm 0.4) \times 10^5 e^2 \text{ fm}^2$ calculated from Eq. (4) is in agreement with the EM value of $(6.11 \pm 0.13) \times 10^5 e^2 \text{ fm}^6$ within uncertainty. A more comprehensive discussion of this topic has been presented elsewhere.⁵¹

In Table III results from a number of medium energy proton experiments are tabulated. It is seen that, with the exception of the 104- and 201-MeV results (but see footnote e to Table III), deformation lengths extracted with the DWBA are apparently constant in energy within an uncertainty of about $\pm 5\%$. The average deformation length extracted is 0.783 ± 0.15 , as compared with the EM value of 0.790 ± 0.008 . We conclude that the collective DWBA formalism is appropriate for intermediate energy proton scattering.

ACKNOWLEDGMENTS

It is a pleasure to acknowledge the considerable assistance of D.A. Hutcheon, R. Abegg, A. Miller, and G. H. McKenzie of the TRIUMF staff. We gratefully acknowledge useful comments by Professor H. Sherif and Professor Vic Madsen. Ken Hicks and O. Häusser helped in gathering the high resolution data and K. Lin assisted with some of the data analysis. This work was supported in part by Oak Ridge National Laboratory, operated by Martin Marietta Energy Systems, Inc. under U.S. Department of Energy Contract DE-AC05-84OR31400, and Los Alamos National Laboratory, operated by the University of California under U.S. Department of Energy Contract W-7405-ENG-36. The University of Oregon and Oregon State University participants were supported in part by grants from the National Science Foundation.

*Present address: Laboratoire National Saturne, Commissariat à l'Énergie Atomique, 91191 Gif-sur-Yvette, Cedex, France.

†Permanent address: Los Alamos National Laboratory, University of California, Los Alamos, NM 87545.

‡Permanent address: University of Lund, Lund, S-223 62, Sweden.

§Permanent address: Oregon State University, Corvallis, OR 97330.

¹C. D. Goodman, in *Proceedings of the 9th International Conference on High Energy Physics and Nuclear Structure, Versailles, 1981*, edited by P. Catillon, P. Radvanyi, and M. Porneuf (North-Holland, Amsterdam, 1982), p. 241.

²K. Takahashi, M. Yamada, and T. Kondoh, *At. Data Nucl.*

Data Tables 12, 101 (1973).

³A. Bohr and B. R. Mottelson, *Phys. Lett.* **100B**, 10 (1981); G. E. Brown and M. Rho, *Nucl. Phys.* **A372**, 397 (1981); T. Izumoto and A. Mori, *Phys. Lett.* **82B**, 169 (1979); E. Oset and M. Rho, *Phys. Rev. Lett.* **42**, 47 (1979).

⁴N. Anantaraman, G. M. Crawley, A. Galonsky, C. Djalali, N. Marty, M. Morlet, A. Willis, and J.-C. Jourdain, *Phys. Rev. Lett.* **46**, 1318 (1981).

⁵D. H. Youngblood, C. M. Rozsa, J. M. Moss, D. R. Brown, and J. D. Bronson, *Phys. Rev. Lett.* **39**, 1188 (1977).

⁶F. E. Bertrand, *Nucl. Phys.* **A354**, 129c (1981); *Annu. Rev. Nucl. Sci.* **26**, 457 (1976).

⁷H. P. Morsch, M. Rogge, R. Turek, and C. Mayer-Böricke,

- Phys. Rev. Lett. **45**, 337 (1980); H. P. Morsch, C. Sükösd, M. Rogge, P. Turek, H. Machner, and C. Mayer-Böricke, Phys. Rev. C **22**, 489 (1980).
- ⁸H. P. Morsch, P. Decowski, M. Rogge, P. Turek, L. Zemlo, S. A. Martin, G. P. A. Berg, W. Hürlimann, J. Meissburger, and J. G. M. Römer, Phys. Rev. C **28**, 1947 (1983).
- ⁹C. Djalali, N. Marty, M. Morlet, and A. Willis, Nucl. Phys. **A380**, 42 (1982).
- ¹⁰T. A. Carey, W. D. Cornelius, N. J. DiGiacomo, J. M. Moss, G. S. Adams, J. B. McClelland, G. Pauletta, C. Whitten, M. Gazzaly, N. Hintz, and C. Glashauser, Phys. Rev. Lett. **45**, 239 (1980).
- ¹¹T. Yamagata, S. Kishimoto, K. Yuasa, K. Iwamoto, B. Saeki, M. Tanaka, T. Fukuda, I. Miura, H. Inoue, and H. Ogoto, Phys. Rev. C **23**, 937 (1981).
- ¹²Michael W. Kirson, Phys. Lett. **108B**, 237 (1982).
- ¹³P. F. Bortignon and R. A. Broglia, Nucl. Phys. **A371**, 405 (1981).
- ¹⁴J. Wambach, V. Klemt, and J. Speth, Phys. Lett. **77B**, 245 (1978); J. Wambach, F. Osterfeld, and J. Speth, Nucl. Phys. **A324**, 77 (1979).
- ¹⁵F. E. Serr, P. F. Bortignon, and R. A. Broglia, Nucl. Phys. **A393**, 109 (1983).
- ¹⁶F. E. Bertrand, in *Studying Nuclei with Medium Energy Protons*, University of Alberta/TRIUMF Workshop, Edmonton, Alberta, 1983, edited by J. M. Greben, TRIUMF publication TRI-83-3, 1983, p. 181.
- ¹⁷G. R. Satchler, Nucl. Phys. **A195**, 1 (1972); G. R. Satchler, in *Proceedings of the International School of Physics, "Enrico Fermi," Course LXIX*, edited by A. Bohr and R. A. Broglia (North-Holland, Amsterdam, 1977), p. 271.
- ¹⁸J. Tinsley, D. K. McDaniels, J. Lisantti, L. W. Swenson, D. M. Drake, R. Liljestrang, F. E. Bertrand, E. E. Gross, D. J. Horen, and T. Sjoreen, Phys. Rev. C **28**, 1417 (1983).
- ¹⁹B. Bonin, N. Alamanos, B. Berthier, G. Bruge, H. Faraggi, D. Legrand, J. C. Lugol, W. Mittag, L. Papineau, A. I. Yavin, D. K. Scott, M. LeVine, J. Arvieux, L. Farvacque, and M. Beunerd, Nucl. Phys. **A430**, 349 (1984).
- ²⁰S. Kailas, P. P. Singh, D. L. Friesel, C. C. Foster, P. Schwandt, and J. Wiggins, Phys. Rev. C **29**, 2075 (1984).
- ²¹F. Osterfeld, J. Wambach, H. Lenske, and J. Speth, Nucl. Phys. **A318**, 45 (1979).
- ²²G. R. Satchler, Nucl. Phys. **A394**, 349 (1983).
- ²³J. Lisantti, J. R. Tinsley, D. M. Drake, I. Bergqvist, L. W. Swenson, D. K. McDaniels, F. E. Bertrand, E. E. Gross, D. J. Horen, and T. P. Sjoreen, Phys. Lett. **147B**, 23 (1984).
- ²⁴F. E. Bertrand, E. E. Gross, D. J. Horen, J. R. Wu, J. Tinsley, D. K. McDaniels, L. W. Swenson, and R. Liljestrang, Phys. Lett. **103B**, 326 (1981).
- ²⁵D. A. Hutcheon, E. D. Copper, P. Kitching, H. S. Sherif, J. M. Cameron, R. P. Liljestrang, C. A. Miller, W. J. McDonald, D. J. Sheppard, W. C. Olsen, G. C. Nielson, J. R. Tinsley, D. K. McDaniels, L. W. Swenson, P. Schwandt, C. E. Stronach, and L. Ray, see Ref. 1, p. 134; D. A. Hutcheon, private communication.
- ²⁶R. A. Arndt, R. H. Hackman, and L. D. Roper, Phys. Rev. C **9**, 555 (1974); R. A. Arndt (unpublished).
- ²⁷All DWBA calculations for $L > 1$ were made with the program ECIS 79, written by J. Raynal (Centre d'Etude Nucléaires de Saclay). The giant monopole and giant dipole calculations were made with the program DWUCK written by P. D. Kunz (University of Colorado).
- ²⁸F. James and M. Roos, Comput. Phys. Commun. **10**, 343 (1975).
- ²⁹B. Jacobsson, A. Brockstedt, and I. Bergqvist, private communication.
- ³⁰H. Sherif and J. S. Blair, Phys. Lett. **26B**, 389 (1968); H. Sherif, Ph.D. thesis, University of Washington, 1968 (unpublished).
- ³¹A. Ingemarsson, E. Hagberg, and H. Sherif, Nucl. Phys. **A216**, 271 (1973).
- ³²A. M. Bernstein, Adv. Nucl. Phys. **3**, 325 (1969).
- ³³M. Gazzaly, N. M. Hintz, G. S. Kyle, R. K. Owen, G. W. Hoffman, M. Barlett, and G. Blanpied, Phys. Rev. C **25**, 408 (1982).
- ³⁴M. J. Martin (unpublished); D. Goutte, J. B. Bellicard, J. M. Cavedon, B. Frois, M. Huet, P. Leconte, Phan Xuan Ho, S. Platchkov, J. Heisenberg, J. Lichtenstadt, C. N. Papanicolas, and I. Sick, Phys. Rev. Lett. **45**, 1618 (1980).
- ³⁵N. Marty, M. Morlet, A. Willis, V. Comparat, and R. Frascaria, Nucl. Phys. **A238**, 93 (1975).
- ³⁶F. Bertrand, E. E. Gross, D. J. Horen, J. Tinsley, D. K. McDaniels, J. Lisantti, L. W. Swenson, K. Jones, T. A. Carey, J. B. McClelland, and S. J. Seestrom-Morris, Phys. Rev. C (in press).
- ³⁷K. Kwiatkowski and N. S. Wall, Nucl. Phys. **A301**, 349 (1978); F. D. Bechetti, Jr. and G. W. Greenless, Phys. Rev. **182**, 1190 (1969).
- ³⁸A. Nadasen, P. Schwandt, P. P. Singh, W. W. Jacobs, A. D. Bacher, P. T. Debevec, M. D. Kaitchuck, and J. T. Meek, Phys. Rev. C **23**, 1023 (1981).
- ³⁹G. R. Satchler, Part. Nucl. **5**, 105 (1973).
- ⁴⁰J. M. Moss, D. H. Youngblood, C. M. Rozsa, D. R. Brown, and J. D. Bronson, Phys. Rev. Lett. **37**, 816 (1976); J. M. Moss, D. R. Brown, D. H. Youngblood, C. M. Rozsa, and J. D. Bronson, Phys. Rev. C **18**, 741 (1978).
- ⁴¹G. Kühner, D. Meuer, S. Müller, A. Richter, E. Spamer, and O. Titze, Phys. Lett. **104B**, 189 (1981); M. Sasao and Y. Torizuka, Phys. Rev. C **15**, 217 (1977).
- ⁴²J. Wambach, V. A. Madsen, G. A. Rinker, and J. Speth, Phys. Rev. Lett. **39**, 1443 (1977).
- ⁴³M. N. Harakeh, B. Van Heyst, K. Van den Borg, and A. Van der Woude, Nucl. Phys. **A327**, 373 (1979).
- ⁴⁴K. F. Liu and G. E. Brown, Nucl. Phys. **A265**, 385 (1976).
- ⁴⁵E. C. Halbert, J. B. McGrory, G. R. Satchler, and J. Speth, Nucl. Phys. **A245**, 189 (1975). This paper contains a theoretical fit to (α, α') data at 13.5°. The 115-MeV alpha scattering experiment was performed by J. M. Moss, C. M. Rozsa, J. D. Bronson, and D. H. Youngblood, Phys. Lett. **538**, 51 (1974).
- ⁴⁶S. Kailas, P. P. Singh, A. D. Bacher, C. C. Foster, D. L. Friesel, P. Schwandt, and J. Wiggins, Phys. Rev. C **26**, 1733 (1982).
- ⁴⁷N. Van Giai and H. Sagawa, Nucl. Phys. **A371**, 1 (1981); R. De Haro, S. Krewald, and J. Speth, Phys. Rev. C **26**, 1649 (1982).
- ⁴⁸V. A. Madsen, F. Osterfeld, and J. Wambach, in *Giant Multipole Resonances*, Proceedings of the Giant Multipole Resonance Topical Conference, Oak Ridge, Tennessee, 1979, edited by F. E. Bertrand (Harwood-Academic, New York, 1980), Vol. 1, p. 93.
- ⁴⁹J. P. Elliot and D. H. Flowers, Proc. R. Soc. (London) **A247**, 57 (1957); G. E. Brown and M. Bolsterli, Phys. Rev. Lett. **3**, 472 (1959).
- ⁵⁰J. Speth, see Ref. 48, p. 33.
- ⁵¹D. K. McDaniels, J. Lisantti, J. Tinsley, I. Bergqvist, L. W. Swenson, F. E. Bertrand, E. E. Gross, and J. Horen, Phys. Lett. **162B**, 277 (1985).
- ⁵²G. S. Adams, A. D. Bacher, G. T. Emery, W. P. Jones, D.

W. Miller, W. G. Love, and F. Petrovich, Phys. Lett. **91B**, 23 (1980).
⁵³V. Comparat, R. Frascaria, N. Marty, M. Morlet, and A. Willis, Nucl. Phys. **A221**, 403 (1974). These authors state

that $\beta_3=0.105$ with $r_I=1.32$ F. Our stated uncertainty corresponds to the difference in $B(E3)$ obtained with $r_I=1.32$ F ($R=r_I A^{1/3}$) and the commonly used mass radius of $1.20 A^{1/3}$.